Exploiting NOMA in D2D Assisted Full-duplex Cooperative Relaying

Tu-Trinh THI NGUYEN, Dinh-Thuan DO

Department of Electronics and Telecommunications, Faculty of Electronics Technology,
Industrial University of Ho Chi Minh City, 12 Nguyen Van Bao, 700000 Ho Chi Minh City, Vietnam

nguyenthitutrinh@iuh.edu.vn, dodinhthuan@iuh.edu.vn

DOI: 10.15598/aeee.v19i3.4116

Article history: Received Feb 20, 2021; Revised Jul 09, 2021; Accepted Jul 20, 2021; Published Sep 30, 2021.

Abstract. *In a wireless system, dual-hop transmission requires Full-Duplex (FD) to transmit signals from the base station too far users. It is more beneficial if we deploy non-orthogonal multiple access to serve specific users, i.e. normal users (near and far users) and device-to-device users. The fairness and outage performance of these users can be studied. We particularly focus on mathematical analysis of outage performance which is computed based on Signal to Noise Ratio (SNR) of received signals at each kind of user. We derive a closed-form formula of such outage probability along with throughput. To realize both the FD NOMA, this paper performs system performance metrics and considers how self-interference make influences system performance. The simulation results validate the theoretical analysis and show that our scheme can obtain a better outage probability and throughput performance with high transmit SNR at the base station and lower required target rates.*

Keywords

NOMA, outage probability, throughput.

1. Introduction

Considering as a prominent approach for the increasing requirements for higher capacity in wireless systems, Non-Orthogonal Multiple Access (NOMA) has recently emerged in the upcoming Fifth-Generation (5G) wireless communications [1], [2], [3], [4], and [5]. To eliminate multi-user interference, the conventional multiple access, namely Orthogonal Multiple Access (OMA), employs orthogonal allocation of resources. The OMA scheme has some kinds, including Time Division Multiple Access (TDMA), Frequency Division Multiple Access (FDMA), and Code Division Multiple Access (CDMA). In principle, multiple users in NOMA can share the same frequency and time resources [6], [7], [8], [9], and [10]. NOMA systems allocate different power levels to different users by changing the level of interference from other users [11].

The wireless systems get benefits from other advances of NOMA systems such as spectral efficiency, low latency, and connectivity which are provided to meet the main requirements of the upcoming 5G wireless communications [12]. However, higher complexity at the receivers using Successive Interference Cancellation (SIC) to eliminate the interference from other users' signals and then detecting their own signals is enabled. By assigning different power levels to different users, NOMA networks exhibit user fairness based on their channel conditions. In particular, users achieve high power coefficients due to their weak channels, while users with stronger channels are assigned with lower power factors.

NOMA with the presence of technologies such as Device-to-Device (D2D) communications provides the heterogeneous nature of 5G cellular systems. The operation of D2D pairs can reuse the spectrum band of cellular users [13], [14], and [15]. The integration of D2D transmission mode into the cellular system makes an interference to broadcast channels or multiple access. In [16] and [17], the application of NOMA in D2D communications has been investigated.

In [18], the authors explored the interplay mode as a special D2D approach for the NOMA system. In such a system, the power domain multiplexing is required for both the D2D pair and cellular users to elimi-

$$|g_{U_1} \leftarrow R|^2 = \Gamma\left(m_{|g_{U_1\leftarrow R}|^2}, \xi_2\alpha_2 \frac{\lambda_{|g_{U_1\leftarrow R}|^2}}{m_{|g_{U_1\leftarrow R}|^2}} + \xi_3\alpha_4 \frac{\lambda_{|g_{U_1\leftarrow R}|^2}}{m_{|g_{U_1\leftarrow R}|^2}}\right) U_1. \quad (1)$$

nate the strong interference between them by the SIC decoding. They presented the case that D2D pair employing the selection between the interplay mode and underlay mode, the SIC decoding constraint is achieved at both D2D receiver and NOMA base station. Reference [19] considered a D2D-enhanced Unmanned Aerial Vehicles (UAV) network, in which D2D is conducted to improve the file dispatching efficiency. Considering such D2D-enhanced UAV systems relying on NOMA, the authors studied graph theory-based algorithms regarding resource allocation. The authors in [20] presented the power allocation sub-problem with continuous variables and decoding order variables. In particular, they first studied a heuristic algorithm to optimize the power allocation for NOMA-based with given D2D power allocation. [21] presented a collaborative protocol with joint power optimization in the D2D-NOMA system. As such, to limit signal leakage, while performing beamforming to suppress AN in the legitimate users' directions, a Full-Duplex (FD) cellular receiver injects the Artificial Noise (AN) signals to deteriorate the eavesdropper's channel. Other merging D2D-NOMA systems can be reported in [21], [22], [23], [24], [25], [26], [27], [28], [29], and [30]. Motivated by work [31], this paper studies performance of D2D groups, in which the near and far users can operate along with D2D users under the context of the NOMA protocol.

2. System Model

In Fig. 1 we consider a downlink NOMA using the dual-hop transmission. In such system, the Base Station (BS) intends to send signals to the near user and the far user, i.e. two cellular users U_1 (near user) and U_2 (far user). Especially, U_2 needs assistance from one full-duplex relay acting user (R) for forwarding signal from BS. In this scenario, a D2D user D_1 is located in serving coverage of such BS. Due to the blockage and hindrance to signal propagation, we cannot process the signal in direct link BS-to U_2 while the remaining links of the NOMA system are available. Benefiting Full-Duplex (FD) mode, the relay re-transmits the decoded symbol only to the far user. Contrarily, in such NOMA, R is able to forward symbol U_2 and its own symbol to D_1 at the same time which is achieved by the enabler of NOMA. In such NOMA system, we examine wireless channels following Nakagami-m fading model. In particular, the channel coefficient experiences Nakagami-m fading will be represented as Gamma distribution with integer fading factor m_z and mean λ_z denoted by $|z|^2 \sim \Gamma\left(m_z, \frac{\lambda_z}{m_z}\right)$.

It is noted that relay R exhibits imperfect Self-Interference (SI) cancellation causing residual at relay $|f|^2 \sim \Gamma\left(m_{|f|^2}, \xi_1 \frac{\lambda_{(|f|^2)}}{m_{(|f|^2)}}\right)$ with $(0 \leq \xi_1 \leq 1)$. At each hop, power levels are reset, i.e. $\alpha_1, \alpha_2, \alpha_3, \alpha_4$ are power allocation coefficients, where $\alpha_1 + \alpha_3 = 1$, $\alpha_1 < \alpha_3$ and $\alpha_2 + \alpha_4 = 1$, $\alpha_2 < \alpha_4$. $\rho_B = \frac{P_B}{\sigma_2^2}$ and $\rho_R = \frac{P_R}{\sigma_2^2}$ are considered as transmit Signal to Noise Ratio (SNR) at the BS and R, with P_B, P_R the total transmit power of BS and the total transmit power of relay, respectively and σ_2^2 is the variance of Additive White Gaussian Noise (AWGN) at R. The channel coefficient of interference link from Eq. (1).

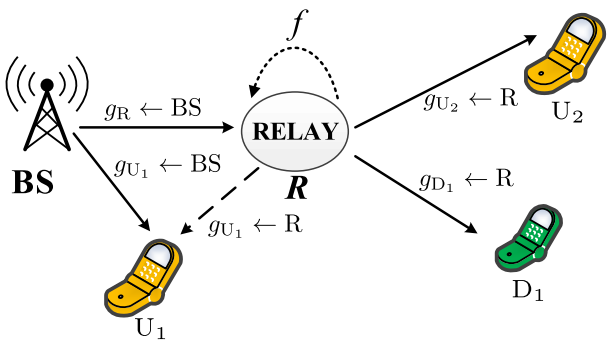

Fig. 1: System model.

Is the level of residual interference $(0 \leq \xi_3 \leq 1)$.

The PDF and CDF of $|g_z|^2$ is given by [33].

$$f_{|z|^2}(x) = \frac{x^{m_z-1}}{\Gamma(m_z)\beta_z^{m_z}} e^{-\frac{x}{\beta_z}}, \quad (2)$$

and

$$F_{|z|^2}(x) = 1 - e^{-\frac{x}{\beta_z}} \sum_{n=0}^{m_z-1} \frac{x^n}{n!\beta_z^n}, \quad (3)$$

where $\beta_z \triangleq \frac{\lambda_z}{m_z}$ with m_z and λ_z represent the integer fading factor and the channel mean power $\lambda_z = E\{|z|^2\}$. $\Gamma(.)$ is the gamma function x is a variable. To further examine system performance metrics, we need to compute Signal-to-Interference-plus-Noise Ratio (SINR). Following the principle of NOMA, the relay is able to decode signal x_3 by considering x_1 as noise and the corresponding SINR at R is formulated

by [31].

$$\gamma_{R\leftarrow BS}^{x_3} = \frac{\alpha_3\rho_B|g_{R\leftarrow BS}|^2}{\alpha_1\rho_B|g_{R\leftarrow BS}|^2 + \rho_R|f|^2 + 1}. \quad (4)$$

To decode signals x_3 and x_1 at U_1, we need to determine the received SINRs respectively as:

$$\gamma_{U_1\leftarrow BS}^{x_3} = \frac{\alpha_3\rho_B|g_{U_1\leftarrow BS}|^2}{\alpha_1\rho_B|g_{U_1\leftarrow BS}|^2 + \rho_R|g_{U_1\leftarrow R}|^2 + 1}, \quad (5)$$

and

$$\gamma_{U_1\leftarrow BS}^{x_1} = \frac{\alpha_1\rho_B|g_{U_1\leftarrow BS}|^2}{\rho_R|g_{U_1\leftarrow R}|^2 + 1}. \quad (6)$$

At the second hop transmission, the far/weak user U_2 receives the signal transmitted from BS and decodes it's information x_3 by treating x_2 as noise. Therefore, the corresponding SINR to detect signal x_3 at U_2 is given by:

$$\gamma_{U_2\leftarrow R}^{x_3} = \frac{\alpha_4\rho_R|g_{U_2\leftarrow R}|^2}{\alpha_2\rho_R|g_{U_2\leftarrow R}|^2 + 1}. \quad (7)$$

Besides two users' signals, D2D user D_1 needs ro receive the transmitted signal from R in this second hop transmission. First, D_1 needs to decode x_3 if treating x_2 as noise. By employing SIC, it can be decoded its own signal x_2. Hence, we can obtain SINRs that correspond correspond to detect x_3 and x_2 at D_1 respectively as:

$$\gamma_{D_1\leftarrow R}^{x_3} = \frac{\alpha_4\rho_R|g_{D_1\leftarrow R}|^2}{\alpha_2\rho_R|g_{D_1\leftarrow R}|^2 + 1}, \quad (8)$$

and

$$\gamma_{D_1\leftarrow R}^{x_2} = \alpha_2\rho_R|g_{D_1\leftarrow R}|^2. \quad (9)$$

The achievable rates of U_1 and D_1 are respectively written by:

$$C_{U_1} = \log_2(1 + \gamma_{U_1^{x_1}} \leftarrow BS), \quad (10)$$

and

$$C_{D_1} = \log_2(1 + \gamma_{D_1^{x_2}} \leftarrow R). \quad (11)$$

Moreover, the achievable rate of U_2 can be obtained by as:

$$C_{U_2} = \log_2(1+\min(\gamma_{R\leftarrow BS}^{x_3}, \gamma_{U_1\leftarrow BS}^{x_3}, \gamma_{U_2\leftarrow R}^{x_3}, \gamma_{D_1\leftarrow R}^{x_3})). \quad (12)$$

Finally, the overall achievable capacity can be calculated as:

$$C_{cap.}^{pro.} = C_{U_1} + C_{D_1} + C_{U_2}. \quad (13)$$

3. Outage Probability Analysis

In this section, it is necessary to determine an important performance metric, i.e. outage probability. Due to differences in terms of power allocation factor and decoding order, such system performance for each user could be different. The definition of outage probability represents probability to SINR less than the specific thresholds which are decided by different demands of users. We first analyze the outage performance of the near user as follow.

3.1. Outage Probability of U_1

Considering the performance metric for the considered system, the Outage Probability (OP) at U_1 can be explained as: Outage behavior will occur in U_1 related to two situations. First, if it can not decode the signal x_3. Second, if it decodes x_3 but it cannot decode x_1. From the above description, the outage probability of U_1 is formulated by:

$$\begin{aligned}\mathcal{P}_{U_1} &= \Pr\left(\begin{array}{l}\log_2\left(1+\gamma_{U_1\leftarrow BS}^{x_3}\right) < R_2,\\ \log_2\left(1+\gamma_{U_1\leftarrow BS}^{x_1}\right) < R_1\end{array}\right)\\ &= \Pr\left(\gamma_{U_1\leftarrow BS}^{x_3} < \delta_2, \gamma_{U_1\leftarrow BS}^{x_1} < \delta_1\right)\\ &= 1 - \Pr\left(\gamma_{U_1\leftarrow BS}^{x_3} \geq \delta_2, \gamma_{U_1\leftarrow BS}^{x_1} \geq \delta_1\right),\end{aligned} \quad (14)$$

where the threshold SNRs are $\delta_1 = 2^{R_1} - 1, \delta_2 = 2^{R_2} - 1$. Substituting the formula Eq. (6) and Eq. (7) into formula Eq. (14) we get:

$$\mathcal{P}_{U_1} = 1 - \Pr\left(\begin{array}{l}A_1\rho_B|g_{U_1\leftarrow BS}|^2 \geq \rho_R|g_{U_1\leftarrow R}|^2 + 1,\\ \frac{\alpha_1}{\delta_1}\rho_B|g_{U_1\leftarrow BS}|^2 \geq \rho_R|g_{U_1\leftarrow R}|^2 + 1\end{array}\right) \quad (15)$$

where $A_1 = \dfrac{\alpha_3 - \alpha_1\delta_2}{\delta_2}$.

The existence of OP reported in (15) is related to situation $\delta_2 > \dfrac{\alpha_3}{\alpha_1}$, the OP becomes $\mathcal{P}_{\mathcal{U}_\infty} = \infty$ and for $\delta_2 < \dfrac{\alpha_3}{\alpha_1}$, the OP can be rewritten by:

$$\mathcal{P}_{U_1} = 1 - \int_0^\infty F_{|g_{U_1\leftarrow BS}|^2}\left[\frac{1}{\varphi\rho_{U_2B}}(\rho_R x + 1)\right] f_{|g_{U_1\leftarrow R}|^2}(x)dx. \quad (16)$$

From formulas Eq. (2) and Eq. (2) we can calculate $F_{|g_{U_1\leftarrow BS}|^2}\left[\dfrac{1}{\varphi\rho_B}(\rho_R x + 1)\right]$ and $f_{|g_{U_1\leftarrow R}|^2}(x)$ as

follows:

$$F_{|g_{U_1\leftarrow BS}|^2}\left[\frac{1}{\varphi\rho_B}\left(\rho_R x+1\right)\right]=1-e^{-\frac{\rho_R x+1}{\varphi\rho_B\beta_{g_{U_1\leftarrow BS}}}}\cdot \cdot\sum_{n=0}^{m_{g_{U_1\leftarrow BS}}-1}\frac{\left(\frac{1}{\varphi\rho_B}\left(\rho_R x+1\right)\right)^n}{n!\beta^n_{g_{U_1\leftarrow BS}}}, \tag{17}$$

$$f_{|g_{U_1\leftarrow R}|^2}(x)=\frac{x^{m_{g_{U_1\leftarrow R}}-1}}{\Gamma\left(m_{g_{U_1\leftarrow R}}\right)}\cdot \cdot\frac{e^{-\frac{x}{\left(\xi_2\alpha_2+\xi_3\alpha_4\right)\beta_{g_{U_1\leftarrow R}}}}}{\left[\left(\xi_2\alpha_2+\xi_3\alpha_4\right)\beta_{g_{U_1\leftarrow R}}\right]^{m_{g_{U_1\leftarrow R}}}}. \tag{18}$$

Substituting Eq. (17) and Eq. (18) into Eq. (16), we get:

$$\mathcal{P}_{U_1}=1-\sum_{n=0}^{m_{g_{U_1\leftarrow BS}}-1}\sum_{k=0}^{n_1}\binom{n_1}{k}e^{-\frac{1}{\varphi\rho_B\beta_{g_{U_1\leftarrow BS}}}}\cdot \cdot\frac{\rho_R^k}{n!\beta^n_{g_{U_1\leftarrow BS}}\varphi^n\rho_B^n\Gamma\left(m_{g_{U_1\leftarrow R}}\right)}\cdot \cdot\frac{1}{\left(\xi_2\alpha_2\beta_{g_{U_1\leftarrow R}}+\xi_3\alpha_4\beta_{g_{U_1\leftarrow R}}\right)^{m_{g_{U_1\leftarrow R}}}}\cdot \cdot\int_0^\infty e^{-\mu x}x^{k+m_{g_{U_1\leftarrow R}}-1}dx, \tag{19}$$

where $\mu\triangleq\frac{\rho_R}{\varphi\rho_B\beta_{g_{U_1\leftarrow BS}}}+\frac{1}{\xi_2\alpha_2\beta_{g_{U_1\leftarrow R}}+\xi_3\alpha_4\beta_{g_{U_1\leftarrow R}}}$ and $\varphi=\min\left(A_1,\frac{\alpha_1}{\delta_1}\right)$.

By using result in [32] and applying some polynomial expansion manipulations, Eq. (19) is computed by:

$$\mathcal{P}_{U_1}=\sum_{n=0}^{m_{g_{U_1\leftarrow BS}}-1}\sum_{k=0}^{n_1}\binom{n_1}{k}\cdot \cdot\frac{\rho_R^k\left(k+m_{g_{U_1\leftarrow R}}-1\right)!}{n!\beta^n_{g_{U_1\leftarrow BS}}\varphi^n\rho_B^n\Gamma\left(m_{g_{U_1\leftarrow R}}\right)}\cdot \cdot\frac{1}{e^{\frac{1}{\varphi\rho_B\beta_{g_{U_1\leftarrow BS}}}}\mu^{k+m_{g_{U_1\leftarrow R}}}\left(\xi_2\alpha_2\beta_{g_{U_1\leftarrow R}}+\xi_3\alpha_4\beta_{g_{U_1\leftarrow R}}\right)^{m_{g_{U_1\leftarrow R}}}}. \tag{20}$$

3.2. Outage Probability of U_2

If R fails to decode x_3 or R can decode but U_2 can not, then outage occurs in U_2. Hence, the OP of U_2 is calculated by:

$$\begin{aligned}\mathcal{P}_{U_2}&=\Pr\left(\begin{array}{l}\log_2\left(1+\gamma^{x_3}_{R\leftarrow BS}\right)<R_2,\\ \log_2\left(1+\gamma^{x_3}_{U_2\leftarrow R}\right)<R_2\end{array}\right)\\&=\Pr\left(\gamma^{x_3}_{R\leftarrow BS}<\delta_2,\gamma^{x_3}_{U_2\leftarrow R}<\delta_2\right)\\&=1-\Pr\left(\gamma^{x_3}_{R\leftarrow BS}\geq\delta_2,\gamma^{x_3}_{U_2\leftarrow R}\geq\delta_2\right).\end{aligned} \tag{21}$$

Replace Eq. (4) and Eq. (7) into Eq. (21), we have:

$$\begin{aligned}\mathcal{P}_{U_2}&=1-\Pr\left(\begin{array}{l}A_1\rho_B|g_{R\leftarrow BS}|^2\geq\rho_R|f|^2+1,\\ \left(\underbrace{\alpha_4-\alpha_2\delta_2}_{\triangleq\wp}\right)\rho_u|g_{U_2\leftarrow R}|^2\geq\delta_2\end{array}\right)\\&=1-\Pr\left(\begin{array}{l}A_1\rho_B|g_{R\leftarrow BS}|^2\geq\rho_R|f|^2+1,\\ \wp\rho_R|g_{U_2\leftarrow R}|^2\geq\delta_2\end{array}\right)\\&=1-\underbrace{\Pr\left(A_1\rho_B|g_{R\leftarrow BS}|^2\geq\rho_R|f|^2+1\right)}_{\triangleq\Psi_1}\cdot\\&\quad\cdot\underbrace{\Pr\left(|g_{U_2\leftarrow R}|^2\geq\frac{\delta_2}{\wp\rho_R}\right)}_{\triangleq\Psi_2}.\end{aligned} \tag{22}$$

If $\delta_2>\frac{\alpha_3}{\alpha_1}$ and $\delta_2>\frac{\alpha_4}{\alpha_2}$ exist, the OP becomes $\mathcal{P}_{U_2}=1$, whereas for $\delta_2<\frac{\alpha_3}{\alpha_1}$ and $\delta_2<\frac{\alpha_4}{\alpha_2}$ it can be expressed:

$$\begin{aligned}\mathcal{P}_{U_2}&=1-\Psi_1\Psi_2\\&=1-\sum_{n=0}^{m_{g_{R\leftarrow BS}}-1}\sum_{k=0}^{n_1}\sum_{n_2=0}^{m_{g_{U_2\leftarrow R}}-1}\binom{n_1}{k}\cdot\\&\quad\cdot\frac{\rho_R^k\left(k+m_f-1\right)!}{n!\beta^n_{g_{R\leftarrow BS}}}\left(\frac{1}{\rho_B A_1}\right)^{n_1}\cdot\\&\quad\cdot\frac{e^{-\frac{1}{\rho_B A_1\beta_{g_{R\leftarrow BS}}}-\frac{\delta_2}{\wp\rho_R\beta_{g_{U_2\leftarrow R}}}}}{\Gamma\left(m_f\right)\left(\xi_1\beta_f\right)^{m_f}}\cdot\\&\quad\cdot\left(\frac{\rho_R}{\rho_B A_1\beta_{g_{R\leftarrow BS}}}+\frac{1}{\xi_1\beta_f}\right)^{-k-m_f}\cdot\\&\quad\cdot\frac{\delta_2^{n_2}}{n_2!\left(\wp\rho_R\beta_{g_{U_2\leftarrow R}}\right)^{n_2}},\end{aligned} \tag{23}$$

where Ψ_1, Ψ_2 can be calculated as follows:

$$\begin{aligned}\Psi_1&\triangleq\mathcal{P}\left(|g_{R\leftarrow BS}|^2\geq\frac{\delta_2}{\rho_B\left(\alpha_3-\alpha_1\delta_2\right)}\left(\rho_R|f|^2+1\right)\right)\\&=\int_0^\infty\left[1-F_{|g_{R\leftarrow BS}|^2}\left(\frac{\rho_R}{\rho_B A_1}x+\frac{1}{\rho_B A_1}\right)\right]\cdot\\&\quad\cdot f_{|f|^2}(x)\,dx.\end{aligned} \tag{24}$$

From Eq. (2) and Eq. (3) we can calculate $F_{|g_{R\leftarrow BS}|^2}\left(\frac{\rho_R}{\rho_B A_1}x+\frac{1}{\rho_B A_1}\right)$ and $f_{|f|^2}(x)$ as follows:

$$\begin{aligned}&F_{|g_{R\leftarrow BS}|^2}\left(\frac{\rho_R}{\rho_B A_1}x+\frac{1}{\rho_B A_1}\right)\\&=1-e^{-\frac{\rho_R}{\rho_B A_1\beta_{R\leftarrow BS}}x}\cdot\\&\cdot e^{-\frac{1}{\rho_B A_1\beta_{R\leftarrow BS}}}\sum_{n=0}^{m_{R\leftarrow BS}-1}\frac{1}{n!\beta_{R\leftarrow BS}^n}\cdot\\&\cdot\left(\frac{\rho_R}{\rho_B A_1}x+\frac{1}{\rho_B A_1}\right)^n,\end{aligned}\tag{25}$$

and

$$f_{|f|^2}(x)\,dx=\frac{x^{m_f-1}}{\Gamma(m_f)\,\beta_f^{m_f}}\exp\left(-\frac{x}{\beta_f}\right).\tag{26}$$

Based on [32] and from the Eq. (24), Eq. (25), Eq. (26), Ψ_1 can be calculated as:

$$\begin{aligned}\Psi_1&=e^{-\frac{1}{\rho_B A_1\beta_{g_{R\leftarrow BS}}}}\cdot\\&\cdot\int_0^\infty\sum_{n=0}^{m_{g_{R\leftarrow BS}}-1}\frac{e^{-\frac{\rho_R}{\rho_B A_1\beta_{g_{R\leftarrow BS}}}x}}{n!\beta_{g_{R\leftarrow BS}}^n}\cdot\\&\cdot\left(\frac{\rho_R}{\rho_B A_1}x+\frac{1}{\rho_B A_1}\right)^n\frac{x^{m_f-1}e^{-\frac{x}{\xi_1\beta_f}}}{\Gamma(m_f)\,(\xi_1\beta_f)^{m_f}}dx\\&=\sum_{n=0}^{m_{g_{R\leftarrow BS}}-1}\sum_{k=0}^{n_1}\binom{n_1}{k}\frac{1}{n!\beta_{g_{R\leftarrow BS}}^n}\cdot\\&\cdot\left(\frac{\rho_R}{\rho_B A_1}\right)^k\left(\frac{1}{\rho_B A_1}\right)^{n_1-k}e^{-\frac{1}{\rho_B A_1\beta_{g_{R\leftarrow BS}}}}\cdot\\&\cdot\int_0^\infty e^{-\frac{\rho_R}{\rho_B A_1\beta_{g_{R\leftarrow BS}}}x}\frac{x^k x^{m_f-1}}{\Gamma(m_f)\,(\xi_1\beta_f)^{m_f}}e^{-\frac{x}{\xi_1\beta_f}}dx.\end{aligned}\tag{27}$$

Based on [32] and applying some polynomial expansion manipulations, Ψ_1 is given by:

$$\begin{aligned}\Psi_1=&\sum_{n=0}^{m_{g_{R\leftarrow BS}}-1}\sum_{k=0}^{n_1}\binom{n_1}{k}\frac{\rho_R^k}{n!\beta_{g_{R\leftarrow BS}}^n}\left(\frac{1}{\rho_B A_1}\right)^{n_1}\cdot\\&\cdot\frac{e^{-\frac{1}{\rho_B A_1\beta_{g_{R\leftarrow BS}}}}(k+m_f-1)!}{\Gamma(m_f)\,(\xi_1\beta_f)^{m_f}}\cdot\\&\cdot\left(\frac{\rho_R}{\rho_B A_1\beta_{g_{R\leftarrow BS}}}+\frac{1}{\xi_1\beta_f}\right)^{-k-m_f}.\end{aligned}\tag{28}$$

Similarly, the following result can be achieved:

$$\begin{aligned}\Psi_2&\triangleq\mathcal{P}\left(|g_{U_2\leftarrow R}|^2\geq\frac{\delta_2}{\wp\rho_R}\right)\\&=e^{-\frac{\delta_2}{\wp\rho_R\beta_{g_{U_2\leftarrow R}}}}\sum_{n_2=0}^{m_{g_{U_2\leftarrow R}}-1}\frac{\delta_2^{n_2}}{n_2!\left(\wp\rho_R\beta_{g_{U_2\leftarrow R}}\right)^{n_2}}.\end{aligned}\tag{29}$$

3.3. Outage Probability of D_1

The two situations to D2D user meet outage behavior which is related to conditions: D_1 fails to decode U_2's signal and D_1 decodes x_3 but fails to decode signal x_2. Therefore, the OP of D_1 is computed as:

$$\begin{aligned}\mathcal{P}_{D_1}&=\Pr\left(\begin{array}{l}\log_2\left(1+\gamma_{D_1\leftarrow R}^{x_3}\right)<R_2,\\\log_2\left(1+\gamma_{D_1\leftarrow R}^{x_2}\right)<R_d\end{array}\right)\\&=\Pr\left(\gamma_{D_1\leftarrow R}^{x_3}<\delta_2,\gamma_{D_1\leftarrow R}^{x_2}<\delta_d\right)\\&=1-\Pr\left(\gamma_{D_1\leftarrow R}^{x_3}\geq\delta_2,\gamma_{D_1\leftarrow R}^{x_2}\geq\delta_d\right).\end{aligned}\tag{30}$$

By replacing Eq. (9) and Eq. (10) into Eq. (30), $\mathcal{P}_{D_1}$ can be recomputed by:

$$\begin{aligned}\mathcal{P}_{D_1}&=1-\Pr\left(\begin{array}{l}\dfrac{\alpha_4\rho_R|g_{D_1\leftarrow R}|^2}{\alpha_2\rho_R|g_{D_1\leftarrow R}|^2+1}\geq\delta_2,\\\alpha_2\rho_R|g_{D_1\leftarrow R}|^2\geq\delta_d\end{array}\right)\\&=1-\Pr\left(\begin{array}{l}|g_{D_1\leftarrow R}|^2\geq\dfrac{\delta_2}{(\alpha_4-\delta_2\alpha_2)\,\rho_R},\\|g_{D_1\leftarrow R}|^2\geq\dfrac{\delta_d}{\alpha_2\rho_R}\end{array}\right)\\&=1-e^{-\frac{\zeta}{\beta_{g_{D_1\leftarrow R}}}}\sum_{n=0}^{m_{g_{D_1\leftarrow R}}-1}\frac{\zeta^n}{n!\beta_{g_{D_1\leftarrow R}}^n}\end{aligned}\tag{31}$$

where $\zeta\triangleq\max\left(\frac{\delta_2}{(\alpha_4-\delta_2\alpha_2)\,\rho_R},\frac{\delta_d}{\alpha_2\rho_R}\right)$.

3.4. Throughput

Based on Eq. (20), throughput of U_1 can be given by:

$$\begin{aligned}\mathcal{T}_{U_1}&=(1-P_{U_1})\,R_1\\&=\left(\begin{array}{l}1-\sum_{n=0}^{m_{g_{U_1\leftarrow BS}}-1}\sum_{k=0}^{n_1}\binom{n_1}{k}\cdot\\\cdot\dfrac{\rho_R^k\,(k+m_{\tilde{g}_{21}}-1)!}{n!\beta_{g_{U_1\leftarrow BS}}^n\varphi^n\rho_B^n\Gamma\left(m_{g_{U_1\leftarrow R}}\right)}\cdot\\\cdot\dfrac{e^{-\frac{1}{\varphi\rho_B\beta_{g_{U_1\leftarrow BS}}}}\mu^{-k-m_{g_{U_1\leftarrow R}}}}{\left(\xi_2\alpha_2\beta_{g_{U_1\leftarrow R}}+\xi_3\alpha_4\beta_{g_{U_1\leftarrow R}}\right)^{m_{g_{U_1\leftarrow R}}}}\end{array}\right)R_1.\end{aligned}\tag{32}$$

From Eq. (23), we have:

$$\mathcal{T}_{U_2} = (1 - \mathcal{P}_{U_2})\, R_2$$

$$= \left(\begin{array}{l} \sum\limits_{n=0}^{m_{g_{R\leftarrow BS}}-1} \sum\limits_{k=0}^{n_1} \sum\limits_{n_2=0}^{m_{g_{U_2\leftarrow R}}-1} \binom{n_1}{k} \cdot \\ \cdot \frac{\rho_R^k\,(k+m_f-1)!}{n!\beta_{g_{R\leftarrow BS}}^n} \left(\frac{1}{\rho_B A_1}\right)^{n_1} \cdot \\ \cdot \frac{e^{-\frac{1}{\rho_B A_1 \beta_{g_{R\leftarrow BS}}} - \frac{\delta_2}{\wp\rho_R \beta_{g_{U_2\leftarrow R}}}}}{\Gamma(m_f)\,(\xi_1\beta_f)^{m_f}} \cdot \\ \cdot \left(\frac{\rho_R}{\rho_B A_1 \beta_{g_{R\leftarrow BS}}} + \frac{1}{\xi_1\beta_f}\right)^{-k-m_f} \cdot \\ \cdot \frac{\delta_2^{n_2}}{n_2!\left(\wp\rho_R\beta_{g_{U_2\leftarrow R}}\right)^{n_2}} \end{array} \right) R_2. \tag{33}$$

Finally, throughput of D_1 can be written as:

$$\mathcal{T}_{D_1} = (1 - \mathcal{P}_{D_1})\, R_d$$

$$= \left(e^{-\frac{\zeta}{\beta_{g_{D_1\leftarrow R}}}} \sum_{n=0}^{m_{g_{D_1\leftarrow R}}-1} \frac{\zeta^n}{n!\beta_{g_{D_1\leftarrow R}}^n} \right) R_d. \tag{34}$$

4. Numerical Results

In this section, we numerically simulate some theoretical results from some figures to show the outage performance. In particular, main parameters can be seen in Tab. 1.

Figure 2 depicts how outage performance can be improved at high transmit SNR $\rho_b = \rho_B$. It can be seen that lower outage probability can be achieved as high SNR. This situation can be explained that high SNR leads to better SINR metrics and then such OP can be enhanced. In the case of fading parameter $m = 2$, the outage performance of the second user outperforms that of the remaining users. The main reason is that different conditions of decoding and power allocation factors lead to different values of OPs for users. By increasing, the quality of wireless channels, $m = 4$ is reported as the best case OP. We can confirm the exactness of derived formulas by matching Monte-Carlo and analytical simulations, i.e. such matching is very tight. The OP performance of user U_1 remains at floor value at high SNR. This can be explained that such OP of user U_1 depends on target rate R_1. We can explain similarly for OP performance of other users at a high region of SNR.

Figure 3 depicts similar trends of OP once we compare cases of target rates R_1, R_2 and R_d. It can be seen that a lower required target rate results in better OP performance for these considered users.

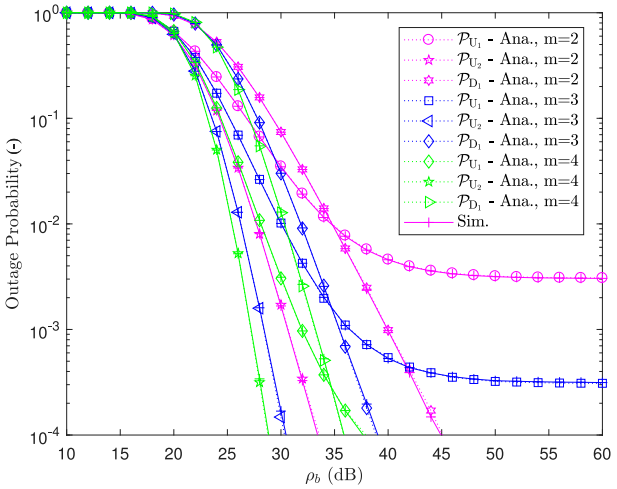

Fig. 2: Outage probability versus transmit SNR with different m.

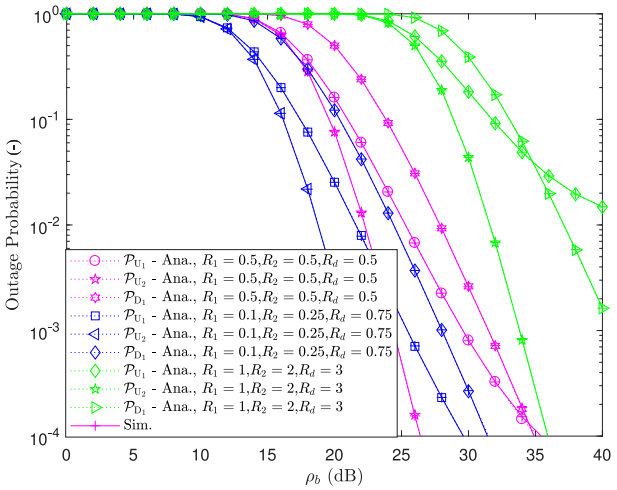

Fig. 3: Outage probability versus transmit SNR with different target rates.

As presented in previous sections, Eq. (4), Eq. (5), Eq. (6), Eq. (7) and Eq. (8) mainly depend on power allocation factors, it is reported in terms of OP performance as Fig. 4. It is still seen that the OP of user U_1 is limited at high SNR. It can be concluded that by reconfiguration for power levels at relay R, we can change how good service to provide to users. The OP performance of different users in NOMA is remarkably improved at high SNR for user U_1 and D2D users. This is a promising result for designing NOMA in a practical scenario. These trends of OP for three users are similar to trends in Fig. 3. As a result, controlling such power factors lead to a crucial impact on performance gaps among three users in such NOMA system. It can be seen that how large amount of self-interference makes influence to outage performance of two users U_1, U_2 as Fig. 5. It can be seen that high ξ_3 leads to worse OP performance. The main reason is that SINR is lower and the corresponding OP will be worse. Especially,

Tab. 1: All parameters in the related simulations.

–	Fig. 2	Fig. 3	Fig. 4	Fig. 5	Fig. 6
R_1 ((bits·s^{-1})Hz^{-1})	1	–	1	1	1
R_2 ((bits·s^{-1})Hz^{-1})	1	–	2	2	1
R_d ((bits·s^{-1})Hz^{-1})	1	–	3	3	1
ϵ_1	0.08^2	0.08^2	0.08^2	–	0.08^2
ϵ_2	1	1	1	–	1
ϵ_3	0.1^2	0.1^2	0.1^2	–	0.1^2
m	–	3	2	2	–
α_1	0.05	0.05	–	0.1	0.05
α_2	0.05	0.05	–	0.1	0.05
α_3	0.95	0.95	–	0.9	0.95
α_4	0.95	0.95	–	0.9	0.95
$\lambda_{g_{U_1}} \leftarrow BS = \lambda_{g_{D_1}} \leftarrow R$	0.01	0.01	0.01	0.01	0.01
$\lambda_{g_R} \leftarrow BS = \lambda_{g_{U_1}} \leftarrow R = \lambda_{g_{U_2}} \leftarrow R$	0.01	0.01	0.01	0.01	0.01
λ_f	0.01	0.01	0.01	0.01	0.01

such outage performance can be very bad in the case of $\xi_3 = 1$. Therefore, limiting the crucial impact of self-interference is a way to improve the system performance.

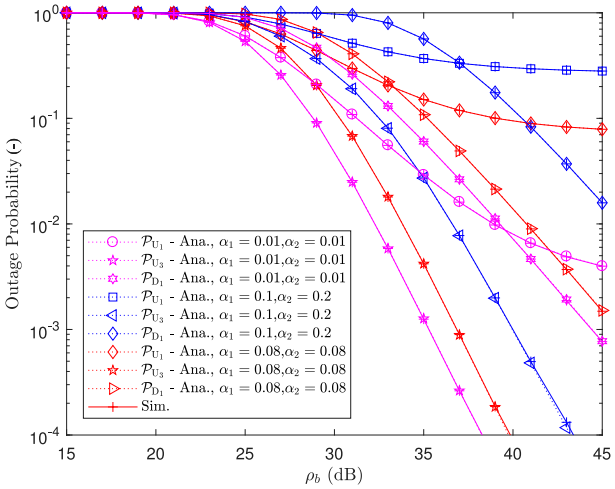

Fig. 4: Outage probability versus transmit SNR with different power allocation factors.

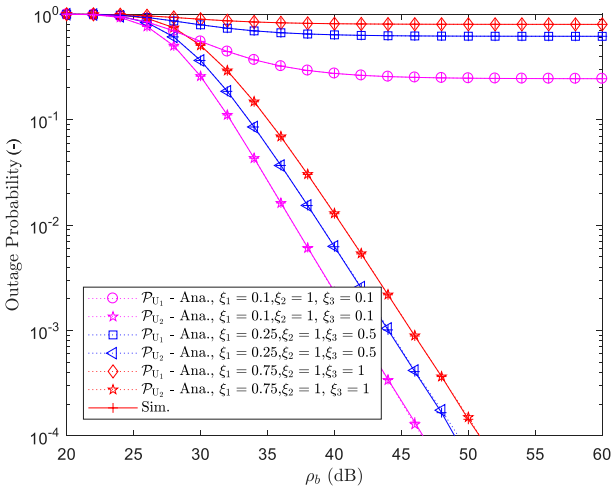

Fig. 5: Outage probability versus transmit SNR with different self-interference levels.

In Fig. 6, we simulate the throughput performance of the proposed scheme versus the transmit SNR at the BS. As shown in previous figures, the OP will be improved significantly at the high region of SNR. As a result, throughput can approach the ceiling value once SNR is greater than 30. By changing channel parameter m, just a slight change can be seen in these throughput curves. Throughput along with OP performance is helpful to give guidelines in the design of NOMA.

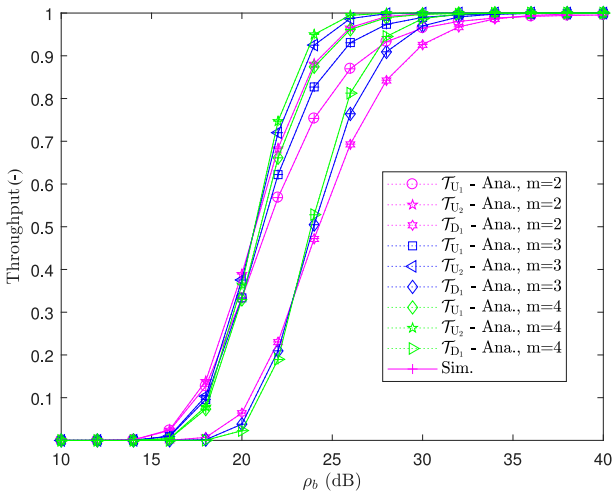

Fig. 6: Throughput performance of U_1, U_2 and D_1.

5. Conclusion

In this paper, we have studied a NOMA adopted at downlink to serve normal users and D2D users. In the proposed scheme, the fixed power allocation approach is adopted along with FD at the relay to improve spectrum efficiency. We considered this meaningful framework to look at outage and throughput performance of many kinds of users, and then employed the NOMA technique to enable the downlink signal processing. For the performance comparison

on these users, we provided a comprehensive analysis of the outage behavior and derived the closed-form expressions of the outage probability. In the following, we consider the different performances of these users. A Nakagami-m fading model was employed to further provide a general case of NOMA. Numerical results are presented to verify the analysis in terms of the outage and throughput performance.

Author Contributions

T.-T.T.N. conceived of the presented idea, developed the theory and performed the computations, developed the theory and performed the computations. D.-T.D. encouraged T.-T.T.N. to investigate [aspecific aspect] and supervised the findings of this work. All authors discussed the results and contributed to the final manuscript. T.-T.T.N. carried out the experiment. D.-T.D. wrote the manuscript with support from A. T.-T.T.N. developed the theoretical formalism, performed the analytic calculations and performed the numerical simulations. Both T.-T.T.N. and D.-T.D. authors contributed to the final version of the manuscript. B. supervised the project. T.-T.T.N. planned and carried out the simulations. T.-T.T.N. and D.-T.D. contributed to the interpretation of the results. B. took the lead in writing the manuscript. All authors provided critical feedback and helped shape the research, analysis and manuscript. T.-T.T.N. designed the model and the computational framework and analysed the data and carried out the implementation and performed the calculations. D.-T.D. wrote the manuscript with input from T.-T.T.N. All authors discussed the results and commented on the manuscript.

References

[1] BARIAH, L., A. AL-DWEIK and S. MUHAIDAT. On the Performance of Non-Orthogonal Multiple Access Systems with Imperfect Successive Interference Cancellation. In: *2018 IEEE International Conference on Communications Workshops (ICC Workshops)*. Kansas City: IEEE, 2018, pp. 1–6. ISBN 978-1-5386-4328-0. DOI: 10.1109/ICCW.2018.8403617.

[2] WANG, B., L. DAI, T. MIR and Z. WANG. Joint User Activity and Data Detection Based on Structured Compressive Sensing for NOMA. *IEEE Communications Letters*. 2016, vol. 20, iss. 7, pp. 1473–1476. ISSN 1558-2558. DOI: 10.1109/LCOMM.2016.2560180.

[3] DO, D.-T. and A.-T. LE. NOMA based cognitive relaying: Transceiver hardware impairments, relay selection policies and outage performance comparison. *Computer Communications*. 2019, vol. 146, iss. 1, pp. 144–154. ISSN 0140-3664. DOI: 10.1016/j.comcom.2019.07.023.

[4] YIN, Y., Y. PENG, M. LIU, J. YANG and G. GUI. Dynamic User Grouping-Based NOMA Over Rayleigh Fading Channels. *IEEE Access*. 2019, vol. 7, iss. 1, pp. 110964–110971. ISSN 2169-3536. DOI: 10.1109/ACCESS.2019.2934111.

[5] ABEBE, A. T. and C. G. KANG. Multiple Codebook-Based Non-Orthogonal Multiple Access. *IEEE Wireless Communications Letters*. 2020, vol. 9, iss. 5, pp. 683–687. ISSN 2162-2345. DOI: 10.1109/LWC.2020.2965939.

[6] ZHU, L., Z. XIAO, X.-G. XIA and D. O. WU. Millimeter-Wave Communications With Non-Orthogonal Multiple Access for B5G/6G. *IEEE Access*. 2019, vol. 7, iss. 1, pp. 116123–116132. ISSN 2169-3536. DOI: 10.1109/ACCESS.2019.2935169.

[7] NGUYEN, T.-L. and D.-T. DO. Power allocation schemes for wireless powered NOMA systems with imperfect CSI: An application in multiple antenna-based relay. *International Journal of Communication Systems*. 2018, vol. 31, iss. 15, pp. 1–17. ISSN 1074-5351. DOI: 10.1002/dac.3789.

[8] DO, D.-T., A.-T. LE and B. M. LEE. On Performance Analysis of Underlay Cognitive Radio-Aware Hybrid OMA/NOMA Networks with Imperfect CSI. *Electronics*. 2019, vol. 8, iss. 7, pp. 1–21. ISSN 2079-9292. DOI: 10.3390/electronics8070819.

[9] LI, X., Q. WANG, H. PENG, H. ZHANG, D.-T. DO, K. M. RABIE, R. KHAREL and C. C. CAVALCANTE. A Unified Framework for HS-UAV NOMA Networks: Performance Analysis and Location Optimization. *IEEE Access*. 2020, vol. 8, iss. 1, pp. 13329–13340. ISSN 2169-3536. DOI: 10.1109/ACCESS.2020.2964730.

[10] DO, D.-T., A.-T. LE and B. M. LEE. NOMA in Cooperative Underlay Cognitive Radio Networks Under Imperfect SIC. *IEEE Access*. 2020, vol. 8, iss. 1, pp. 86180–86195. ISSN 2169-3536. DOI: 10.1109/ACCESS.2020.2992660.

[11] SHIN, W., M. VAEZI, B. LEE, D. J. LOVE, J. LEE and H. V. POOR. Non-Orthogonal Multiple Access in Multi-Cell Networks: Theory, Performance, and Practical Challenges. *IEEE Communications Magazine*. 2017, vol. 55, iss. 10, pp. 176–183. ISSN 1558-1896. DOI: 10.1109/MCOM.2017.1601065.

[12] DAI, L., B. WANG, Y. YUAN, S. HAN, I. CHIH-LIN and Z. WANG. Non-orthogonal multiple access for 5G: solutions, challenges, opportunities, and future research trends. *IEEE Communications Magazine*. 2015, vol. 53, iss. 9, pp. 74–81. ISSN 1558-1896. DOI: 10.1109/MCOM.2015.7263349.

[13] LEI, L., Z. ZHONG, C. LIN and X. SHEN. Operator controlled device-to-device communications in LTE-advanced networks. *IEEE Wireless Communications*. 2012, vol. 19, iss. 3, pp. 96–104. ISSN 1558-0687. DOI: 10.1109/MWC.2012.6231164.

[14] BOCCARDI, F., R. W. HEATH, A. LOZANO, T. L. MARZETTA and P. POPOVSKI. Five disruptive technology directions for 5G. *IEEE Communications Magazine*. 2014, vol. 52, iss. 2, pp. 74–80. ISSN 1558-1896. DOI: 10.1109/MCOM.2014.6736746.

[15] ASADI, A., Q. WANG and V. MANCUSO. A Survey on Device-to-Device Communication in Cellular Networks. *IEEE Communications Surveys* & Tutorials. 2014, vol. 16, iss. 4, pp. 1801–1819. ISSN 1553-877X. DOI: 10.1109/COMST.2014.2319555.

[16] LIU, Y. and E. ERKIP. Capacity and Rate Regions of a Class of Broadcast Interference Channels. *IEEE Transactions on Information Theory*. 2016, vol. 62, iss. 10, pp. 5556–5572. ISSN 1557-9654. DOI: 10.1109/TIT.2016.2519029.

[17] ZHAO, J., Y. LIU, K. K. CHAI, Y. CHEN and M. ELKASHLAN. Joint Subchannel and Power Allocation for NOMA Enhanced D2D Communications. *IEEE Transactions on Communications*. 2017, vol. 65, iss. 11, pp. 5081–5094. ISSN 1558-0857. DOI: 10.1109/TCOMM.2017.2741941.

[18] DAI, Y., M. SHENG, J. LIU, N. CHENG, X. SHEN and Q. YANG. Joint Mode Selection and Resource Allocation for D2D-Enabled NOMA Cellular Networks. *IEEE Transactions on Vehicular Technology*. 2019, vol. 68, iss. 7, pp. 6721–6733. ISSN 1939-9359. DOI: 10.1109/TVT.2019.2916395.

[19] WANG, B., R. ZHANG, C. CHEN, X. CHENG, L. YANG, H. LI and Y. JIN. Graph-Based File Dispatching Protocol With D2D-Enhanced UAV-NOMA Communications in Large-Scale Networks. *IEEE Internet of Things Journal*. 2020, vol. 7, iss. 9, pp. 8615–8630. ISSN 2327-4662. DOI: 10.1109/JIOT.2020.2994549.

[20] CHEN, J., J. JIA, Y. LIU, X. WANG and A. H. AGHVAMI. Optimal Resource Block Assignment and Power Allocation for D2D-Enabled NOMA Communication. *IEEE Access*. 2019, vol. 7, iss. 1, pp. 90023–90035. ISSN 2169-3536. DOI: 10.1109/ACCESS.2019.2926438.

[21] WANG, J., Y. HUANG, S. JIN, R. SCHOBER, X. YOU and C. ZHAO. Resource Management for Device-to-Device Communication: A Physical Layer Security Perspective. *IEEE Journal on Selected Areas in Communications*. 2018, vol. 36, iss. 4, pp. 946–960. ISSN 1558-0008. DOI: 10.1109/JSAC.2018.2825484.

[22] CHEN, Y., X. JI, K. HUANG, B. LI and X. KANG. Opportunistic access control for enhancing security in D2D-enabled cellular networks. *Science China Information Sciences*. 2018, vol. 61, iss. 4, pp. 1–12. ISSN 1869-1919. DOI: 10.1007/s11432-017-9160-y.

[23] SHALMASHI, S. and S. B. SLIMANE. Cooperative device-to-device communications in the downlink of cellular networks. In: *2014 IEEE Wireless Communications and Networking Conference (WCNC)*. Istanbul: IEEE, 2014, pp. 2265–2270. ISBN 978-1-4799-3083-8. DOI: 10.1109/WCNC.2014.6952682.

[24] ZHANG, G., K. YANG, P. LIU and J. WEI. Power Allocation for Full-Duplex Relaying-Based D2D Communication Underlaying Cellular Networks. *IEEE Transactions on Vehicular Technology*. 2015, vol. 64, iss. 10, pp. 4911–4916. ISSN 1939-9359. DOI: 10.1109/TVT.2014.2373053.

[25] SUN, L., Q. DU, P. REN and Y. WANG. Two Birds With One Stone: Towards Secure and Interference-Free D2D Transmissions via Constellation Rotation. *IEEE Transactions on Vehicular Technology*. 2016, vol. 65, iss. 10, pp. 8767–8774. ISSN 1939-9359. DOI: 10.1109/TVT.2015.2505715.

[26] WANG, L., H. WU and G. L. STUBER. Cooperative Jamming-Aided Secrecy Enhancement in P2P Communications With Social Interaction Constraints. *IEEE Transactions on Vehicular Technology*. 2017, vol. 66, iss. 2, pp. 1144–1158. ISSN 1939-9359. DOI: 10.1109/TVT.2016.2553121.

[27] JIANG, L., C. QIN, X. ZHANG and H. TIAN. Secure beamforming design for SWIPT in cooperative D2D communications. *China Communications*. 2017, vol. 14, iss. 1, pp. 20–33. ISSN 1673-5447. DOI: 10.1109/CC.2017.7839755.

[28] KIM, J.-B., I.-H. LEE and J. LEE. Capacity Scaling for D2D Aided Cooperative Relaying Systems Using NOMA. *IEEE Wireless Communications Letters*. 2018, vol. 7, iss. 1, pp. 42–45. ISSN 2162-2345. DOI: 10.1109/LWC.2017.2752162.

[29] XING, T., N. MA and P. ZHANG. Joint Channel Assignment and Power Allocation for NOMA-based D2D Communications with Imperfect CSI. In: *2019 11th International Conference on Wireless Communications and Signal Processing (WCSP)*. Xian: IEEE, 2019, pp. 1–6. ISBN 978-1-72813-555-7. DOI: 10.1109/WCSP.2019.8928004.

[30] LEE, S., J. KIM and S. CHO. Resource Allocation for NOMA based D2D System Using Genetic Algorithm with Continuous Pool. In: *2019 International Conference on Information and Communication Technology Convergence (ICTC)*. Jeju: IEEE, 2019, pp. 705–707. ISBN 978-1-72810-893-3. DOI: 10.1109/ICTC46691.2019.8939884.

[31] UDDIN, M. B., M. F. KADER and S. Y. SHIN. Exploiting NOMA in D2D assisted full-duplex cooperative relaying. *Physical Communication*. 2020, vol. 38, iss. 1, pp. 1–10. ISSN 1874-4907. DOI: 10.1016/j.phycom.2019.100914.

[32] GRADSHTEYN, I. S. and I. M. RYZHIK. *Table of Integrals, Series, and Products*. 6th ed. Cambridge: Academic press, 2000. ISBN 978-0-12-294757-5.

[33] XIANG, Z., W. YANG, Y. CAI, J. XIONG, Z. DING and Y. SONG. Secure Transmission in a NOMA-Assisted IoT Network With Diversified Communication Requirements. *IEEE Internet of Things Journal*. 2020, vol. 7, iss. 11, pp. 11157–11169. ISSN 2327-4662. DOI: 10.1109/JIOT.2020.2995609.

About Authors

Tu-Trinh THI NGUYEN received the B.Sc. degree in electrical-electronics engineering from the Industrial University of Ho Chi Minh City, Vietnam, in 2018. She intends to pursue her study in the Ph.D. degree. She is currently working with the Wireless Communications Laboratory (WiCom) Laboratory, which has lead by Dr. Thuan. Her research interests include signal processing in wireless communications networks, Non-orthogonal Multiple Access (NOMA), and relaying networks.

Dinh-Thuan DO (Senior Member, IEEE) received the B.Sc., M.Sc., and Ph.D. degrees from Vietnam National University (VNU-HCM), in 2003, 2007, and 2013, respectively, all in communications engineering. Prior to joining Ton Duc Thang University, he was a Senior Engineer with VinaPhone Mobile Network, from 2003 to 2009. He has published over 75 SCI/SCIE journal articles, one sole author book, and five book chapters. His research interests include signal processing in wireless communications networks, cooperative communications, non-orthogonal multiple access, full-duplex transmission, and energy harvesting. He was a recipient of the Golden Globe Award from the Vietnam Ministry of Science and Technology, in 2015 (Top 10 Excellent Young Scientists Nationwide). He has been serving as an Associate Editor for six journals, in which main journals are European Association for Signal Processing (EURASIP) Journal on Wireless Communications and Networking, Computer Communications (Elsevier), and the Korean Society for Internet Information (KSII) Transactions on Internet and Information Systems.